Structure, Vol. 10, 1677–1686, December, 2002, ©2002 Elsevier Science Ltd. All rights reserved. PII S0969-2126(02)00909-7

The Crystal Structure of the Hexadeca-Heme Cytochrome Hmc and a Structural Model of Its Complex with Cytochrome c_3

Mirjam Czjzek,[1,3] Latifa ElAntak,[2] Véronique Zamboni,[1] Xavier Morelli,[2] Alain Dolla,[2] Françoise Guerlesquin,[2] and Mireille Bruschi[2]

[1]Architecture et Fonction des Macromolécules Biologiques

[2]Unité de Bioénergétique et Ingénierie des Proteines

IBSM-CNRS et Université Aix-Marseille I et II

31 Chemin Joseph-Aiguier

13402 Marseille cedex 20

France

Summary

Sulfate-reducing bacteria contain a variety of multi-heme *c*-type cytochromes. The cytochrome of highest molecular weight (Hmc) contains 16 heme groups and is part of a transmembrane complex involved in the sulfate respiration pathway. We present the 2.42 Å resolution crystal structure of the *Desulfovibrio vulgaris* Hildenborough cytochrome Hmc and a structural model of the complex with its physiological electron transfer partner, cytochrome c_3, obtained by NMR restrained soft-docking calculations. The Hmc is composed of three domains, which exist independently in different sulfate-reducing species, namely cytochrome c_3, cytochrome c_7, and Hcc. The complex involves the last heme at the C-terminal region of the V-shaped Hmc and heme 4 of cytochrome c_3, and represents an example for specific cytochrome-cytochrome interaction.

Introduction

Sulfate-reducing bacteria are present day representatives of bacteria catalyzing a very ancient process, the biological reduction of sulfur compounds in anaerobic environments, which has been reported to occur as far back as 3.5 Gyrs [1]. Molecular hydrogen plays a central role in the metabolic activity of many sulfate-reducing *Desulfovibrio* species. A peculiar class of molecules, the low-redox potential multi-heme cytochromes *c*, has an important function in hydrogen metabolism. The best characterized of these cytochromes is the tetra-heme cytochrome c_3 (Mr 13,000) [2] (further on referred to as cytochrome c_3), which can be considered as the structural basic unit of the cytochrome c_3-type superfamily members [3], namely the cytochrome c_3 fold. The establishment of the first complete genome of the sulfate-reducing bacteria *Desulfovibrio vulgaris* Hildenbourough (*Dv*H; www.tigr.org) revealed that there are four c_3-type cytochromes and several other multi-heme cytochromes. One may suppose that the presence of this large number of multi-heme cytochromes in these bacteria is a direct consequence of their adaptability to environmental changes, so that each cytochrome would be involved in a metabolic pathway under particular conditions.

Another multi-heme *c*-type cytochrome, called Hmc, has been well characterized in *Dv*H [4–6]. Hmc is a periplasmic high-molecular weight cytochrome that contains 16 heme groups in a single polypeptide chain. Biochemical studies have established that 15 of the hemes are low spin, while the sixteenth is high spin [5, 6]. Although Hmc has been described as being composed of several c_3-like domains [7], experimental evidence clearly shows that it did not play the same role as cytochromes c_3, since Hmc is reduced by periplasmic hydrogenases in a very inefficient way. However, the addition of cytochrome c_3 greatly activates its reduction by hydrogenases. Cytochrome c_3 could thus act as an electron shuttle between hydrogenases and Hmc [8, 9].

The gene encoding Hmc is the first gene of an operon that encodes a transmembrane redox complex (the Hmc complex) composed of six proteins [10]. This complex has been shown to link the periplasmic hydrogen oxidation to the cytoplasmic sulfate reduction pathway [11]. The periplasmic location of Hmc has long been debated, since it has also been isolated in nonnegligible amounts from membrane fractions. Interfacial studies on Hmc with lipid monolayers, however, have demonstrated that it is capable of strong interactions with membranes, but not of integrating in them [12]. It is now well established that it is a periplasmic cytochrome, capable of interacting with membrane-bound electron transfer partners [13]. Thus, its physiological role can be considered as an electron transfer gate between the periplasmic-soluble cytochromes and the membrane-bound electron transfer complex. It remains unclear why this cytochrome contains 16 hemes to fulfill its role.

Despite well-known biophysical properties, no structural information is available on this 16-heme-containing cytochrome. We report here the first crystal structure of the Hmc from *Dv*H, revealing its modular organization in three domains. Subsequently, the combination of NMR titration using ^{15}N-labeled cytochrome c_3 with a docking calculation was performed in order to determine the interacting site of Hmc with the soluble cytochrome c_3, one of its physiological partners.

Results and Discussion

Overall Structural Description

Fully oxidized Hmc crystallized in the space group $P6_2$. The crystal structure was determined using a combination of molecular replacement and multiwavelength anomalous dispersion (MAD) at the Fe absorption edge. One molecule occupies the asymmetric unit. Electron density is observed for residues 10–512 and the 16 heme

[3]Correspondence: czjzek@afmb.cnrs-mrs.fr

Key words: multi-heme cytochrome; heme packing; crystal structure; NMR; sulfate-reducing bacteria; electron transfer complex

Table 1. Summary of Crystallographic Statistics

Data sets	Native	λ_1	λ_2
Wavelength (Å)	0.93	1.73891	1.74135
High resolution (Å)	2.42	2.50	2.60
Completeness (%)	99.4 (99.2)[a]	96.8 (84.0)	98.7 (92.0)
Redundancy	7.6 (7.5)	5.0 (3.2)	5.2 (3.6)
$I/\sigma(I)$	6.5 (1.5)	9.4 (2.0)	9.3 (2.1)
R_{sym}[b]	0.061 (0.331)	0.059 (0.366)	0.056 (0.319)
Phasing statistics			
Dispersive/anomalous difference (%)	—/3.6	9.4/8.8	11.5/6.3
Figure of merit (overall)	0.739 (0.788)[c]		
Refinement statistics			
R_{cryst} (%)[d]	20.3		
R_{free} (%)[e]	27.8		
Rms deviation bond lengths (Å)	0.039		
Rms deviation bond angles	3.37°		

[a] Numbers in parentheses indicate values for the highest resolution bin.
[b] $R_{sym} = \Sigma[|i - \langle I \rangle|]/\Sigma[\langle I \rangle]$, where i is the ith measurement and $\langle I \rangle$ is the weighted mean of I.
[c] Figure of merit value in parentheses is calculated after density modification with DM.
[d] $R_{cryst} = \Sigma||F_{obs}| - |F_{calc}||/\Sigma|F_{obs}|$
[e] R_{free} is the same as R_{cryst} for 5% of the data omitted from refinement totaling 1281 reflections.

groups. All residues in the model are positioned in well-defined density, except residues 470–476, a small surface loop, which is partially disordered, and the side chains of Q144 and R512, which have been truncated to alanines. The current model, refined at 2.42 Å resolution, has an R factor of 20.3% and an R_{free} of 27.8%, and good geometry (Table 1).

The overall structure of Hmc may be described as being composed of three domains (Figure 1). The 16 hemes are numbered according to the sequential appearance of the covalent cysteine linkages from heme 601–616. The N-terminal domain I, including residues K10–P112 and hemes 601–603, is highly homologous to the three-heme-containing cytochrome c_7 from *Desulfuromonas acetoxidans* [14], with a root-mean-square deviation (rmsd) of 2.13 Å for 65 out of 68 C_α atoms. The second domain, domain II, from G122–A223, covalently linking hemes 604–607, highly resembles the cytochromes c_3 (rmsd of 2.65 Å for 88 out of 110 C_α positions), while the C-terminal domain III, from R236–R512, has the same spatial arrangement as the nona-heme cytochrome Hcc (rmsd of 1.01 Å for 229 out of 290 C_α atoms), the structure of which has recently been determined [15]. This third Hcc-like domain, as previously described [15–17], is furthermore constituted of two subdomains, both having the typical cytochrome c_3 fold, and an insertion linking an isolated heme group, heme 611 in Hmc.

The modular organization of Hmc reveals that this redox protein most probably was derived by the acquisition of several multi-heme cytochromes. Another example that may be cited, where domain acquisition has led to a modular organization, is hydrogenases, which have acquired a ferredoxin-like domain [18]. The modular organization is detectable at the level of primary sequence, as has been proposed earlier by Pollock et al. [7]. The overall description based on the sequence, that the Hmc was composed of one c_7- and three c_3-like domains and one isolated heme group, was good, however the positioning of the isolated heme, which is heme 611 (or heme 11), was wrong. As a consequence, the positioning of the high-spin heme was also erroneous. This has already been corrected by the sequence comparison with the nine-heme-containing Hcc [16]. Matias et al. [16] proposed that the high-spin heme was heme 15 (heme 615 for Hmc numbering) rather than heme 12, based on their sequence alignment. Our structure determination definitely shows that this assumption was correct, the third domain being highly homologous to Hcc, heme 611 is the isolated heme, and heme 615 is the high-spin heme.

Interestingly, the overall arrangement of the three domains gives the Hmc a V-shaped form with no intramolecular contacts between the c_7-like N-terminal domain and the Hcc-like C-terminal domain. Therefore, a heme chain running from the N-terminal to the C-terminal can be defined (Figure 2). At each end of the V-shaped cytochrome, a heme corresponding to a heme 4 of the cytochrome c_3 fold (hemes 603 and 616) is exposed to the molecular surface. The orientation and arrangement of the hemes within each domain of the Hmc cytochrome are very similar to those characteristic of all multi-heme cytochromes with the cytochrome c_3 fold [19]: hemes 1 and 4 are approximately parallel, both almost perpendicular to hemes 2 and 3, which are again mutually perpendicular. The global heme arrangement throughout the Hmc polypeptide chain, the inter-heme Fe-Fe distances, as well as the correspondence of the heme groups to those of the cytochrome c_3 fold are schematized in Figure 2. The heme edge-to-edge distances of neighboring heme groups in the c_3-type heme arrangement are rather short, ranging from 3.5 Å (between hemes 601 and 607) and 7.4 Å (between hemes 614 and 616) in Hmc. The edge-to-edge distance barrier for efficient electron transfer between redox centers in proteins has been established by Page and coworkers to be about 14 Å [20]. The histidine plane angles and the surface accessibility of the different heme groups are given in Table 2. As a consequence of being at domain interfaces, the surface exposure of hemes 601, 604, and 608 in Hmc are substantially diminished. Interestingly, the surface exposure of heme 607 (corresponding to a heme 4 of the cytochrome c_3 fold) at the interface of the c_3-like

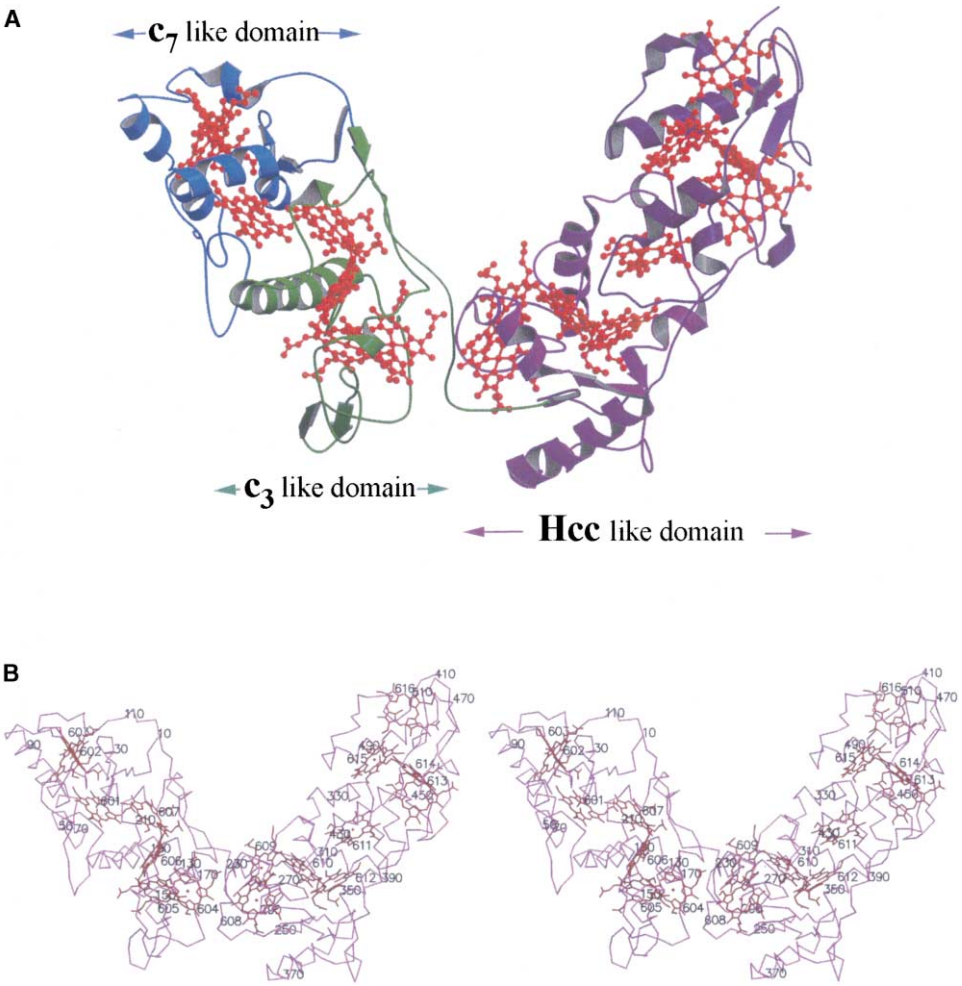

Figure 1. The Crystal Structure of the Hmc Cytochrome

(A) Ribbon representation of the Hmc structure. All heme groups are in red, while the three modules are color coded in blue (c_7-like domain), green (c_3-like domain), and purple (Hcc-like domain).

(B) Eye-walled stereo Cα trace of the Hmc structure. Every twentieth residue is numbered, as well as all the heme groups. Figures 1, 4, and 7 were produced with Molscript [43] and Raster3D [44].

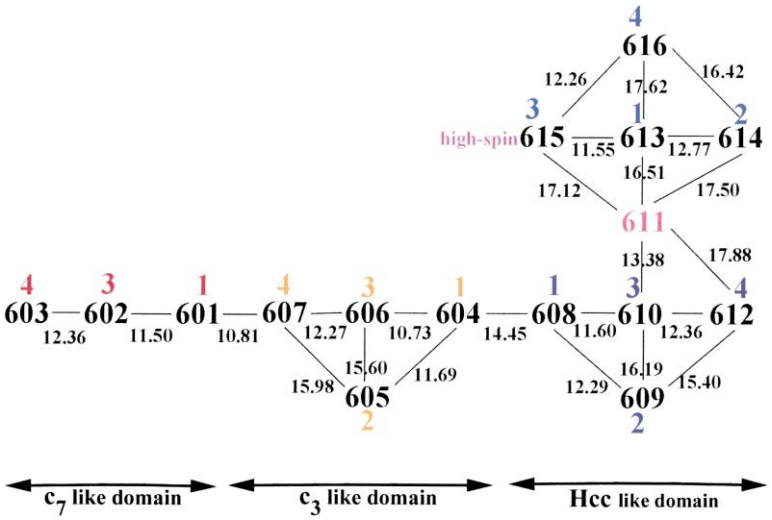

Figure 2. Schematic Description of the Heme Packing Arrangement in Cytochrome Hmc

The inter-heme Fe-Fe distances (in black) between the hemes, sequentially numbered from 601 to 616, are given for distances closer than 18 Å. The colored numbers indicate the correspondence of the heme groups of the different domains (c_7-like domain in red; c_3-like domain in yellow; N-terminal subdomain of the Hcc-like domain in dark blue; C-terminal subdomain of the Hcc-like domain in blue) to the four-heme cluster typically observed in the cytochrome c_3 fold.

Table 2. His-Plane Angles and Solvent-Accessible Surface of the Heme Groups of Hmc Compared to c_7 from *D. acetoxidans*, c_3 from *Dv*H, and Hcc from *D. desulfuricans* ATCC27774

Heme in Hmc	His-plane angle (°)[a]	Surface exposure (Å²)[b]	Heme in cytochrome	His-plane angle (°)[a]	Surface exposure (Å²)[b]
601	26.8	74	1 in c_7	67.8	172
602	12.9	131	2 in c_7	26.5	197
603	91.9	109	3 in c_7	92.9	237
604	29.2	30	1 in c_3	0.5	146
605	79.9	181	2 in c_3	64.2	185
606	18.7	106	3 in c_3	8.7	183
607	91.5	138	4 in c_3	7.5	138
608	38.4	74	1 in Hcc	30.4	174
609	34.1	145	2 in Hcc	38.4	235
610	18.4	79	3 in Hcc	27.7	52
611	27.3	55	4 in Hcc	9.6	21
612	23.4	103	5 in Hcc	26.5	130
613	91.3	84	6 in Hcc	29.9	119
614	1.1	210	7 in Hcc	2.2	204
615	—	164	8 in Hcc	27.4	117
616	19.1	106	9 in Hcc	42.8	95

[a] Angle between the planes of the two histidines, and the fifth and sixth ligands of each heme iron atom.
[b] The solvent-accessible surface was calculated with TURBO [41] using an H_2O probe radius of 1.6 Å.

and the Hcc-like domains, has not changed. Another remarkable observation is that the heme exposure to the solvent for all hemes of the c_7-like domain is lower than that observed in the soluble cytochrome c_7, while the other heme groups have comparable surface exposures as the equivalent heme groups in the isolated cytochromes c_3 and Hcc.

The particular heme packing arrangement of this cytochrome together with its V-shaped form are a new argument in favor of the hypothesis of Barker and Ferguson [21], who proposed that covalent attachment of heme groups in *c*-type cytochromes might serve, besides the economy of minimizing the amino acid residue to heme ratio, to position hemes within a protein. Here, it clearly serves to enable a unique and very dense packing arrangement (the heme to amino acid ratio is 1:32 for Hmc) of 16 hemes within one polypeptide chain, a packing that most probably could not be established by other means. In this type of multi-heme cytochrome the hemes may be considered as analogous to conventional protein structural elements [21], holding the ensemble tightly together, and conferring thermal stability to the overall protein fold [22].

Some particular features are worth mentioning: the N-terminal domain, like cytochrome c_7 from *Desulforomonas acetoxidans*, lacks heme 2 of the four-heme cluster, typical for the cytochrome c_3 fold; as mentioned before [16], one isolated heme group (heme 611) separates two tetra-heme arrangements within the C-terminal nine-heme-containing domain. Another peculiarity of this latter domain is the presence of the high-spin heme (heme 615; Figure 3A), where the iron atom has only five ligands. This is a unique feature of cytochrome Hmc within the multi-heme cytochrome family of *Desulfovibrio* species. However, penta-coordinated high-spin hemes have been observed in other *c*-type multi-heme cytochromes, such as cytochrome c_{554} [23] and hydroxylamine oxidoreductase [24], where the high-spin heme is supposed to be involved in catalytic reactions, giving a bifunctional role to these cytochromes: at the same time enzymes and electron carriers. As in the mentioned examples, the unligated face of the heme group is protected against solvent by stacking interactions with hydrophobic residues; in the case of Hmc, Phe416, Pro417, and Ile421. No water molecule takes the place of the axial ligand in this structure. Due to the presence of this high-spin heme in Hmc, detected by EPR measurements [5], enzymatic activities have been explored [6] but no physiological function for these potential enzymatic activities of Hmc has been elucidated to date. All other heme groups of Hmc display the typical bishistidinyl coordination, in part responsible for the low redox potentials of cytochromes c_3 ranging from −100 mV to −400 mV.

Despite the high homology of the different domains to the cytochrome c_3 fold and the perfectly superposable heme clustering in groups of three or four (with one exception: heme 611), the polypeptide chain also displays several important differences and insertions with respect to the classical c_3 fold. Two of these insertions, a loop insertion in the c_3-like domain II from V153 to W163 and the connection between the two subdomains of the Hcc-like domain III, including residues V352–L395 (see also Figure 3B), come to lie close to the apex of the "V." These two loops contain several hydrophobic and aromatic residues, rather unusually exposed to the surface of the molecule, which therefore seem to form an ideal hydrophobic patch for the interaction with membrane-bound electron transfer partners.

Interdomain Interactions within Hmc and Crystal Packing

The modular arrangement of the Hmc cytochrome has the advantage of offering a structural basis to analyze cytochrome-cytochrome interacting surfaces, which have so far been accessible only in crystal packing contacts. Remarkably, both domain interfaces within Hmc have counterparts in crystal contacts of cytochromes c_3 and involve different structural features and heme groups.

The interdomain contact between domains I and II involves heme 601 and heme 607, respectively (Figure

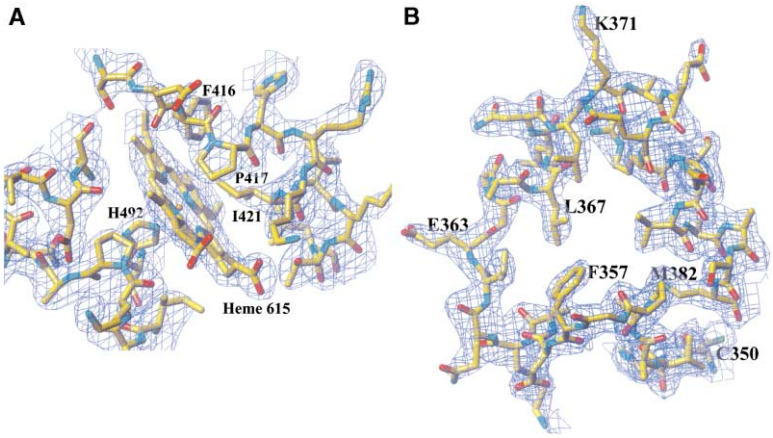

Figure 3. Sections of the Final $2F_o - F_c$ Map

(A) Electron density map in the region of the high-spin heme 615, showing that no sixth ligand is present at this heme. The $2F_o - F_c$ map is contoured at a 1σ level. An isoleucine, a proline, and a phenylalanine are tightly packed against the heme group, protecting the hydrophobic heme cavity from the solvent. No water molecules are observed in the cavity, even though this heme group is highly exposed to the surface (164 Å^2) in the same manner as all heme groups in this cytochrome fold.

(B) Electron density map showing the quality of the map in the region of a highly solvent-exposed surface loop (the loop includes residues 350–359; the density includes residues C350–M382). The $2F_o - F_c$ map is contoured at a 1σ level.

4A). Therefore, the interface brings heme 1 of the cytochrome c_7-like domain I close to the equivalent of heme 4 of domain II. A similar heme 1-heme 4 interaction has been observed in the crystal packing contacts of cytochrome c_3 from *Desulfomicrobium norvegicum* [2]. On the basis of these crystal contacts, supported by the fact that these cytochromes are conducting in the solid phase [25], it had been postulated that an incoming electron would follow the intramolecular electron pathway through hemes 4-3-1 [26, 27]. The here observed arrangement of the c_7-like domain with respect to the c_3-like domain is in favor of this hypothesis; the heme chain follows the sequence 4-3-1 through both domains.

The di-heme stacking arrangement at the domain interface is a parallel but offset packing along the edge of pyrrole rings A and B, closely related to that observed in many other heme packing arrangements [28]. The offset, however, is not only lateral but vertical, in a way that pyrrole ring A of heme 601 is closest to pyrrole ring B of heme 607 (edge-to-edge distance 601 C3A-607 CBB 3.8 Å). This heme stacking has the peculiarity of bringing the histidines, sixth iron ligands of hemes 601 and 607 respectively, close to the edge of the contacting heme (His35 $C^{\epsilon 1}$-607 CBB 3.6 Å and His191 C^{γ}-601 CMA 3.7 Å). Interestingly, the intermolecular heme Fe-Fe distance is on the short side (10.81 Å) of typical intramolecular heme iron-iron distances in the cytochrome c_3 fold, which are in the range of 10.5 to 17.9 Å.

In contrast, the interface between domains II and III involves hemes 604 and 608, which are hemes equivalent to heme 1 in the cytochrome c_3 fold (Figure 4B). The contact between two hemes 1 at the interface of multi-heme cytochrome domains has already been observed in the interface of the homodimeric octa-heme cytochrome cc_3 [29]. However, the relative heme arrangement is closer to perpendicular (the angle between the heme planes is $\sim$130°) than parallel. This "magic angle" between heme planes is equally often observed in electron transfer chains involving heme groups; other examples are the photosynthetic reaction center [30] and cytochrome c_{554} [28]. The closest contact between the respective heme edges is 3.9 Å (between 604 CMA and 608 CMB), and the iron-to-iron distance is 14.5 Å.

The crystal packing is an arrangement of three crystallographic "dimers" around the 6_2-fold axis. In these "dimers," the Hmc molecules are oriented head to tail with the N-terminal domain facing the C-terminal domain, leaving a rectangular open space about 19 Å wide and 40 Å large. None of the crystal packing interfaces in the crystals of Hmc involve intermolecular close heme-

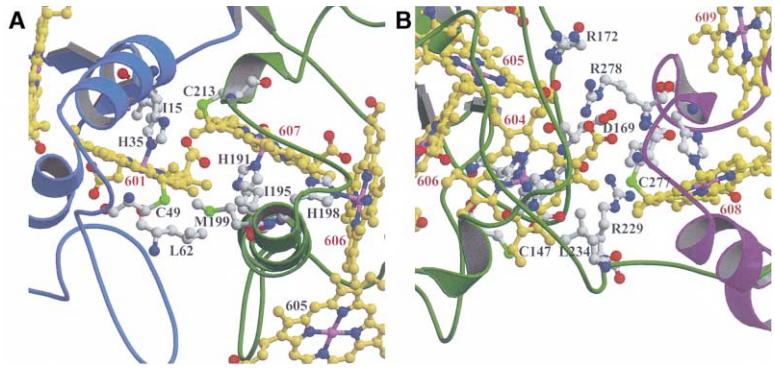

Figure 4. Ribbon Representation of the Interdomain Interactions within Hmc

(A) The interface between the c_7-like and the c_3-like domain involves hemes 601 and 607. The hemes are almost parallel, but offset in a manner that brings the propionate group of heme 601 in hydrogen binding distance of His191, sixth axial ligand of heme 607 (distance His191 $N^{\delta 1}$-Heme 601 O2A = 3.76 Å). The free imidazole nitrogen ($N^{\delta 1}$) of His35, sixth axial ligand of heme 601, in contrast, is in short distance to S^{γ} of Cys213 (3.61 Å), which covalently links heme 607. Otherwise, the interface mainly involves hydrophobic residues, such as Ile15, Leu62, and I195. A short sulfur-sulfur distance (3.7 Å) bridging the interface is observed for Cys49 and Met199.

(B) The interface between the c_3-like and the Hcc-like domains involves hemes 604 and 608. Here, a rather high number of charged residues, such as Asp169, Glu168, Arg172, Arg229, and Arg278, as well as one propionate group of heme 604, are at the interface. Interestingly, one clear-cut salt bridge is formed between Arg278 and O1A of the propionate group of heme 604 (2.82 Å).

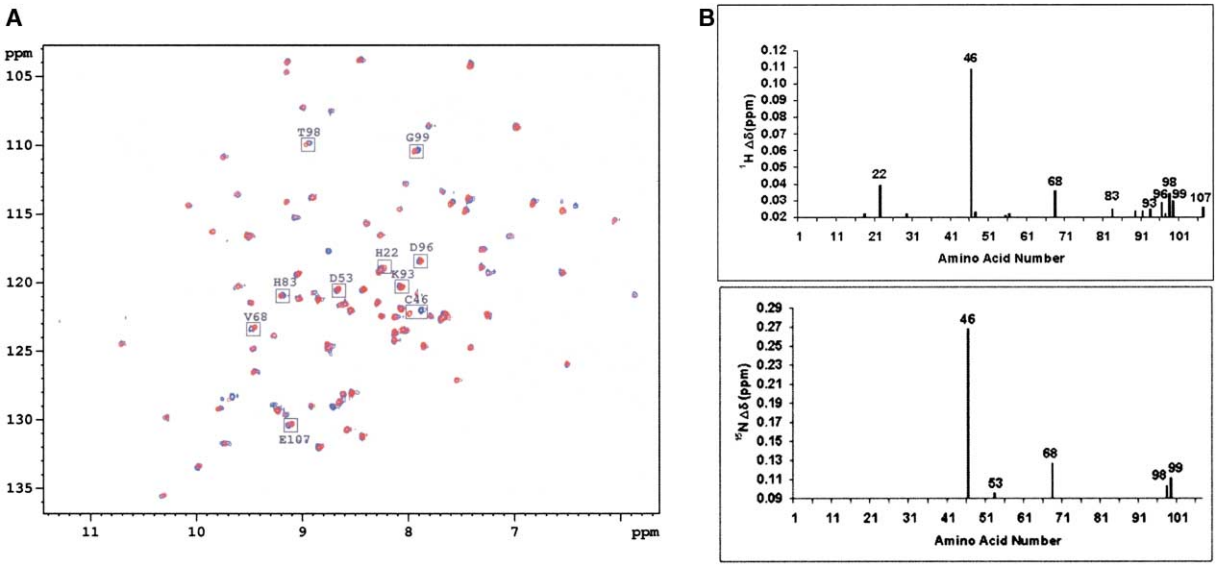

Figure 5. NMR HSQC Spectra of Cytochrome c_3 in the Absence and Presence of Hmc

(A) Superimposition of the ^{1}H-^{15}N spectra of cytochrome c_3 uncomplexed (blue peaks) and complexed with cytochrome Hmc at a ratio of 1:1 (red peaks). Boxes identify crosspeaks (labeled with residue assignments) that have undergone chemical shift variations after complexation. The concentration of cytochrome c_3 was 11 μM in 10 mM potassium phosphate (pH 5.9), in 90% H_2O/10% D_2O. The spectra were recorded at 296 K in the presence of 0 and one equivalent of Hmc.

(B) The chemical shift variation of the ^{1}H and ^{15}N resonances induced by the presence of Hmc. The ten most significant amino acids are selected to constitute the NMR filter, resulting in the NMR constraints: residues 22, 46, 53, 68, 83, 93, 96, 98, 99, and 107.

heme contacts, in contrast to those observed in the crystals of the other multi-heme cytochromes [2, 14, 27, 29]. The shortest intermolecular heme iron-iron distance between Hmc molecules is about 23 Å.

Structural Model of the Complex Cytochrome c_3-Hmc

Biochemical studies have shown that Hmc interacts rather specifically with cytochrome c_3 [8, 9]. The crystallization of such complexes, however, remains inaccessible due to the low affinities of the redox proteins. Recently, we have developed a strategy to study solution complexes between redox partners by combining a soft-docking calculation with NMR experimental data [31–33]. We have successfully applied this approach to the study of the complex between Hmc and cytochrome c_3.

Amino acids of the cytochrome c_3 involved in the interaction with the cytochrome Hmc were determined by recording ^{1}H-^{15}N HSQC experiments and analyzing ^{1}H and ^{15}N chemical shift variations (Figures 5A and 5B). Ten residues are affected by the complex formation. These NMR constraints were used to filter the 1000 ab initio docking solutions determined by BiGGER (Figure 6A) [34]. Interestingly, we find that some red spheres, representing the solutions with the highest BiGGER scores, are concentrated and clustered in three regions: (1) in the C-terminal region, interacting with the Hcc-like domain, (2) interacting with the Hcc-like domain but at the opposite extremity compared to the previous one, and (3) interacting with the cytochrome c_7-like domain. These three regions apparently display common features recognized by the docking algorithm, and therefore may represent potential interaction sites for different physiological partners of Hmc.

After NMR filtering of the 1000 ab initio complex solutions, the solutions were ranked according to the level of agreement with the NMR data. Ten complex solutions presented an NMR score (number of NMR constraints respected) higher than 4 and are therefore considered to be in agreement with the NMR data. Then these ten solutions were scored according to the inter-heme Fe-Fe distances within the docked complexes. Four complex solutions have Fe-Fe distances shorter or equal to 14 Å, while the distance is more than 17 Å for the six other solutions, compatible with the NMR data. The corresponding heme edge-to-edge distances are around 6 and 10 Å, respectively. Both are therefore largely in the range of distances required for electron tunneling, as determined by Page and coworkers, who have established the edge-to-edge distance barrier to be at about 14 Å [20]. However, considering the significant gap between the four solutions with shorter distances and the six other solutions, the complex solutions involving shorter contacts will clearly be more efficient. The four solutions having the shortest heme edge-to-edge distances were therefore selected to be further considered. All four solutions are grouped at the C-terminal end of domain III (the first region mentioned above; Figure 6B) and in fact involve the same interface, differences being due to rotations less than 5° with respect to the complex interface. Since electron transfer complexes are generally not highly specific, it has been suggested that several relative orientations of the two partner molecules are possible [32, 35]. The four solutions found here would therefore represent slightly different docking possibilities between these two molecules. The two other regions, detected by the docking algorithm, are incompatible with the NMR experimental data obtained for

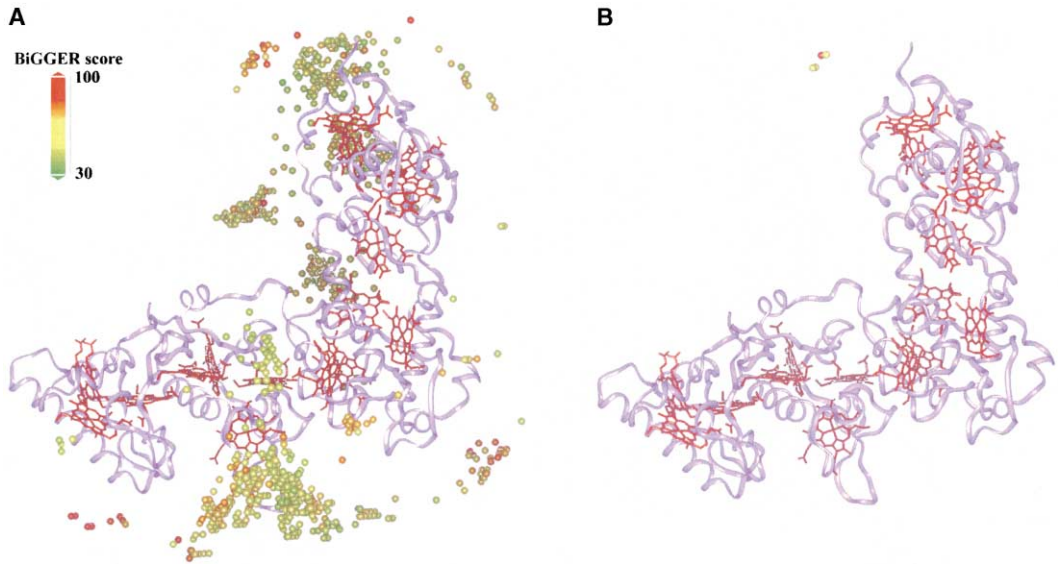

Figure 6. Results of the Docking of the Cytochrome c_3-Hmc Complex after Ab Initio Calculations and NMR Filtering

(A) The backbone of Hmc is represented as a violet ribbon and its 16 hemes are colored in red. Each sphere represents the center of mass of the cytochrome c_3 for each solution. After ab initio calculations, 1000 solutions were generated and ranked according to the interacting scoring function. The 1000 spheres representing the obtained solutions are color coded to reflect the BiGGER score.

(B) Four of the ten solutions present a distance smaller than 17 Å, in agreement with an effective electron transfer, and involve heme 4 of the cytochrome c_3 and heme 616 of the cytochrome Hmc. The four spheres representing those solutions are color coded to indicate the NMR constraints respected (the solution represented by a red sphere respects five constraints and the yellow ones respect four). NMR filtering retains the four solutions located in the C-terminal region. The figure was produced with the BiGGER software package [34].

cytochrome c_3 in the presence of Hmc. The solution with the best NMR and BiGGER score is represented in Figure 7A. The accessible surface area buried at the interface is about 1107 Å^2, approximately 550 Å^2 on each cytochrome. This is a rather low percentage of the overall surface for the Hmc molecule (2.3%), but in the typical range for cytochrome c_3 (9%). However, in view of the V-shaped form of the Hmc molecule and the fact that it is composed of several domains, the small size of the buried interface is not surprising. The composition of

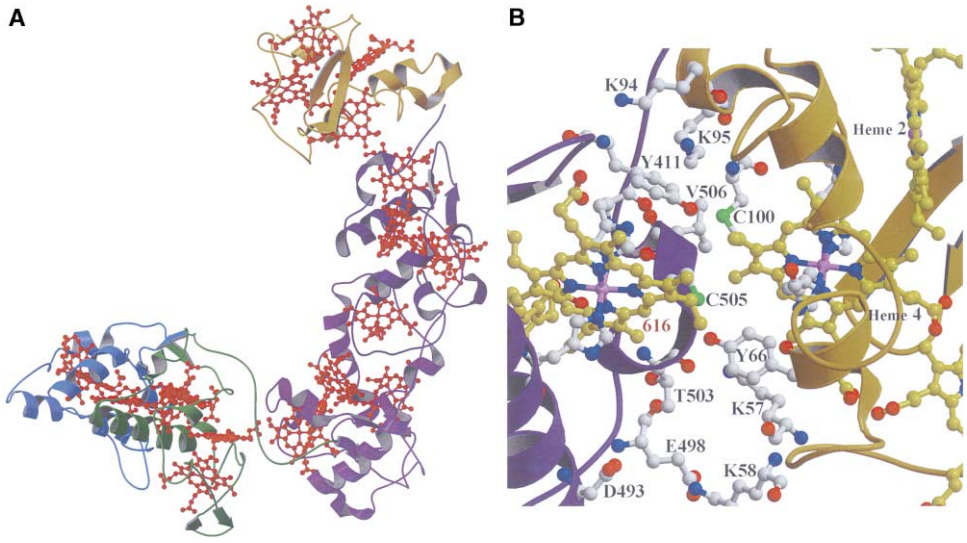

Figure 7. The Structural Model of the Complex between Hmc and Cytochrome c_3

(A) Ribbon representation of the structural solution of the complex having the best docking as well as the best NMR scores. The Hmc domains are color coded in blue, green, and violet as previously, while the cytochrome c_3 is in yellow.

(B) A close-up view of the interface between the C-terminal domain of Hmc and cytochrome c_3. A close sulfur-sulfur distance (4.2 Å) involves Cys505, linking heme 616 of Hmc, and C100, linking heme 4 of cytochrome c_3. Two tyrosine residues make hydrogen bonds across the interface. The lysines surrounding the heme 4 crevice of cytochrome c_3 are facing negatively charged residues at the interface of Hmc. Despite this, no direct salt bridges are formed across the interface in this structural model.

the interface is very typical for electron transfer complexes [35], with about 37% polar and 63% apolar atoms at the interface (values obtained at the protein-protein interaction server http://www.biochem.ucl.ac.uk/bsm/PP/server/). A docking model of the complex between cytochrome c_3 and the nona-heme cytochrome Hcc has recently been proposed [15]. However, in that case, the interacting region of the selected solution was close to the N-terminal hemes of Hcc, equivalent to the region involved in the domain interface between the c_3-like domain II and the Hcc-like domain III for Hmc. In the same manner as for Hmc, several patches around the oval-shaped molecule Hcc had been located by the docking calculation between cytochrome c_3 and nona-heme cytochrome Hcc in *Desulfovibrio desulfuricans* ATCC 27774 [15]. The most important patches are located at the N- and C-terminal regions of Hcc. The authors had chosen solutions at the N-terminal end, since they had the highest scores by the docking algorithm. Our experience has shown that for most low-affinity redox complexes, the power of the docking algorithms is limited and experimental data are necessary to select correct solutions. It is noteworthy that both patches of docking solutions between cytochrome c_3 and Hcc correspond to interacting regions of the Hcc-like domain in Hmc: the N-terminal region interacts with the c_3-like domain within the Hmc molecule and the C-terminal region forms the interface in the complex cytochrome c_3-Hmc in our results.

Here, the interface between the complexed molecules involves heme 4 of cytochrome c_3 and heme 616 of cytochrome Hmc, and most likely represents the physiological electron transfer site for this particular complex (Figure 7B). The interface brings the cysteine residues, which covalently link the hemes in van der Waals contact. This is a feature in common with several recently determined electron transfer complexes [32, 36]. The sulfur atom of C100, covalently linking heme 4 in cytochrome c_3, is at a distance of 4.2 Å to the sulfur of C505 linking heme 616. Another common feature to the previously examined complexes are hydrophobic and tyrosine residues at the interface. Here, V506 of the Hmc is in close contact with the surface-exposed hydrophobic heme edge (pyrrole ring B), similar to the highly conserved I36 of the [Fe]-hydrogenase in the complexes with either cytochrome c_{553} [32] or cytochrome c_3 [36]. In the same way as in the complex with [Fe]-hydrogenase, Y66 of cytochrome c_3 forms a hydrogen bond with the main chain carbonyl of T503 of Hmc. A second tyrosine, this time Y411 of Hmc, is also close to the interacting surface.

It is well known that electron transfer complexes are, in the first place, driven by electrostatic forces. In the complex presented here, lysine residues of loops 1 and 4 of cytochrome c_3 (loops defined in [28]) are indeed at the interface of the complex, mostly interacting with acidic residues from Hmc. However, most of these lysine residues are not directly involved in salt bridges.

Most interestingly, the interacting surface of cytochrome c_3 with the [Fe]-hydrogenase [36] and Hmc are identical, involving heme 4 in both cases. Five out of ten and 11 residues, respectively, affected in the NMR spectra for these two complexes, are in common (C46, D53, D96, T98, and G99). This observation has the direct consequence that cytochrome c_3, which is believed to shuttle electrons from one partner to the other, cannot interact with both at the same time. Another consequence is that only one out of four heme groups of cytochrome c_3 interacts with the physiological partners. This brings us back to the question, why the multi-heme cytochromes *c* contain several heme groups. Three reasons may be retained as possible explanations: the necessity of electron storage, the electron transfer of multiple electron pairs in the reduction of sulfate, and/or the observed thermal stability of these redox proteins. More exciting is the question concerning the role of the modular organization in three domains, based on different natures of multi-heme cytochromes, in the V-shaped Hmc. The modular aspect of this cytochrome may be due to an evolutionary development. The unit base is represented by the four-heme-containing cytochrome c_3 that itself has been described as originating from gene duplication [37]. Larger cytochromes would be obtained by the variation of this unit by either oligomerization, which is the case for the homodimeric cytochrome cc_3, or by domain acquisition as for the nona-heme cytochromes Hcc or the 16-heme-containing Hmc. The modular organization of the Hmc presented here may relate to an evolutionary advantage in that this cytochrome could interact with several different redox partners as a function of environmental conditions. The presence of several cytochromes c_3 in the periplasm has only been established recently, when the complete genome of *Desulfovibrio vulgaris* Hildenborough has been sequenced. One can imagine that these different cytochromes c_3 interact at the different sites, observed in the docking calculations, of cytochrome Hmc. Herein the two wings of the V-shaped cytochrome might even be independently functioning electron transfer pathways: the distance separating heme 604 in domain II and heme 608 in domain III is 14.5 Å, which is longer than the typical range of iron-iron distances observed in these cytochromes. This would implicate that the region at the base of the "V" serves to interact and shuttle electrons to the membrane-bound redox partners of the *hmc* operon. This hypothesis is supported by the fact that the base region of the "V" indeed contains highly surface exposed aromatic residues, such as Tyr154 and Phe357, located in surface-exposed loops of the c_3-like domain II and the Hcc-like domain III, respectively, and might play key roles for the interaction with membrane-bound transfer proteins. Further investigations in order to ascertain these hypotheses will be performed in future studies.

Biological Implications

Sulfate-reducing bacteria are present day representatives of bacteria catalyzing a very ancient process, the biological reduction of sulfur compounds in anaerobic environments. Molecular hydrogen plays a central role in the metabolic activity of many *Desulfovibrio* species. Hydrogenases catalyze the heterolytic cleavage of molecular hydrogen producing electrons and protons, while multi-heme *c*-type cytochromes are of crucial importance for electron transfer. In *Desulfovibrio vulgaris* Hildenborough, two types of multi-heme cytochromes *c* have been characterized: tetra-heme cytochromes c_3

and the hexadeca-heme Hmc, which is the largest *c*-type cytochrome so far documented. They are part of a unique system, both cytochromes of type *c* being involved in the same transport chain electronically connecting the periplasmic hydrogen oxidation to the cytoplasmic sulfate reduction. In this system the tetra-heme cytochrome c_3 acts as an electron shuttle between the hydrogenase and Hmc.

Our results reveal that the hexadeca-heme Hmc can be described as three independent modules, most probably derived from domain acquisition. The modular organization in the form of a "V" of the here presented Hmc may relate to an evolutionary advantage in that this cytochrome could interact with several different redox partners as a function of environmental conditions. Herein the two wings of the V-shaped cytochrome might even be independently functioning electron transfer pathways, representing the entrance gates to the transfer across the membrane, since Hmc is the first of six redox proteins of a transmembrane electron transfer complex. Subsequent to the structure determination, the formation of the complex with the physiological partner cytochrome c_3 was measured by NMR, showing that the C-terminal heme (heme 616) of Hmc interacts with heme 4 of cytochrome c_3 at the complex interface. The same interacting surface of cytochrome c_3 has been observed in the complex, with hydrogenase having as a consequence that these three components of the transfer chain cannot interact simultaneously.

Experimental Procedures

Crystallization

The expression and purification of wild-type Hmc has been described elsewhere [5]. Even though some purification steps were handled in anaerobic conditions, the crystallization trials of Hmc were treated aerobically, and the cytochrome was therefore in the fully oxidized state during the structure determination. Crystals of Hmc were grown in 24-well Limbro plates by vapor diffusion using the hanging drop method. The 0.5 ml well solution contained 30% Jeffamine M-600, 50 mM cesium chloride, and 100 mM 2-morpholinoethanesulfonic acid (MES) (pH 6.5). The 4 μl drop contained 2 μl of cytochrome at a concentration of 6 mg ml^{-1} and 2 μl of well solution. A single crystal grew within several months to a size of $0.3 \times 0.3 \times 0.1$ mm^3. The crystal belonged to the hexagonal space group P 6_2 with unit cell dimensions a = b = 108.4 Å and c = 102.8 Å, and contained one monomer per asymmetric unit, corresponding to a Matthews volume V_M of 2.73 $Å^3$ Da^{-1}.

Data Collection and Phasing

The X-ray diffraction data sets from the native protein crystal were collected on ID14-EH2 at λ = 0.93 Å and on ID29 at two wavelengths close to the iron absorption edge (i.e., at the absorption peak λ = 1.73891 and the inflection point λ = 1.74135). All data were collected at 100 K, on the same crystal. Data were processed and integrated with DENZO [38] and scaled using SCALA of the CCP4 [39] suite. The first nine iron positions were determined by the molecular replacement solution of the C-terminal domain with the Hcc nine-heme-containing search model. The residual maps after preliminary phasing by these nine iron positions using SHARP [40] revealed the missing seven iron atoms. The iron atom parameters were refined and final phases were calculated with SHARP. The figure of merit (FOM) was 0.74 at this stage. Phasing was further improved by solvent flattening and histogram matching with the subroutine DM from the CCP4 [39] suite leading to a final FOM value of 0.79.

Model Building and Refinement

The model was manually built into the MAD-phased electron density map, starting with the highly homologous Hcc as a model using TURBO-FRODO [41]. Cycles of model improvement and refinement were then performed alternately using TURBO-FRODO and Refmac5/CCP4, respectively. The refinement and addition of water molecules was terminated at the point where R_{free} began to increase.

NMR Experiments and Filtering of the Docking

^{15}N-labeled cytochrome c_3 from *Dv*H was obtained as previously described [42]. ^{15}N-^{1}H HSQC experiments were recorded on a Bruker Avance DRX500 spectrometer equipped with an HCN probe. Spectra were acquired accumulating 224 scans per free induction decay, with 256 complex points in F1 and 2K complex points in F2. Processing and spectra analysis were done with XwinNMR from Bruker. ^{15}N and ^{1}H chemical shift assignments of cytochrome c_3 have been previously reported (accession number BMRB-5239).

The protein coordinates of *Dv*H cytochrome c_3 were obtained from the Protein Data Bank (2cth). Molecular interaction simulations were executed using the docking program BiGGER [34]. This algorithm performs a complete and systematic search in the binding space of both molecules. A population of 1000 candidates of cytochrome c_3-Hmc docked geometries is generated. Putative docked structures are ranked using an interaction scoring function. NMR filtering of the 1000 ab initio solutions is obtained by using ^{15}N and ^{1}H chemical shift variations that were observed in HSQC experiments performed on cytochrome c_3 in the absence and presence of Hmc, and which are therefore correlated to the complex formation. These variations are converted into distance parameters, considering that ^{1}H and ^{15}N chemical shifts of an amide group are affected if the concerned atom is at least at 5 Å from any atom belonging to the interacting partner.

Acknowledgments

This research was supported by the CNRS. We thank A. Roussel for help during data collection, M. Woudstra for protein purification, as well as R. Toci of the fermentation plant for the growth of bacteria. We are indebted to the ESRF staff, who have helped during data collections.

Received: May 16, 2002
Revised: September 19, 2002
Accepted: September 20, 2002

References

1. Shen, Y., Buick, R., and Canfield, D.E. (2001). Isotopic evidence for microbial sulphate reduction in the early Archaean era. Nature *410*, 77–81.
2. Czjzek, M., Payan, F., Guerlesquin, F., Bruschi, M., and Haser, R. (1994). Crystal structure of cytochrome c_3 from *Desulfovibrio desulfuricans* Norway at 1.7 Å resolution. J. Mol. Biol. *243*, 653–667.
3. Bruschi, M. (1994). Cytochrome c_3 (M(r) 26,000) isolated from sulfate-reducing bacteria and its relationships to other polyhemic cytochromes from *Desulfovibrio*. Methods Enzymol. *243*, 140–155.
4. Higuchi, Y., Yasuoka, N., Kakudo, M., Katsube, Y., Yagi, T., and Inokuchi, H. (1987). Single crystals of hydrogenase from *Desulfovibrio vulgaris* Miyazaki F. J. Biol. Chem. *262*, 2823–2825.
5. Bruschi, M., Bertrand, P., More, C., Leroy, G., Bonicel, J., Haladjian, J., Chottard, G., Pollock, W.B., and Voordouw, G. (1992). Biochemical and spectroscopic characterization of the high molecular weight cytochrome c from *Desulfovibrio vulgaris* Hildenborough expressed in *Desulfovibrio desulfuricans* G200. Biochemistry *31*, 3281–3288.
6. Verhagen, M.F., Pierik, A.J., Wolbert, R.B., Mallee, L.F., Voorhorst, W.G., and Hagen, W.R. (1994). Axial coordination and reduction potentials of the sixteen hemes in high-molecular-mass cytochrome c *from Desulfovibrio vulgaris* (Hildenborough). Eur. J. Biochem. *225*, 311–319.
7. Pollock, W.B., Loutfi, M., Bruschi, M., Rapp-Giles, B.J., Wall, J.D., and Voordouw, G. (1991). Cloning, sequencing, and expression of the gene encoding the high-molecular-weight cytochrome c from *Desulfovibrio vulgaris* Hildenborough. J. Bacteriol. *173*, 220–228.
8. Pereira, I., Romao, C.V., Xavier, A.V., Legall, J., and Teixiera, M.

(1998). Electron transfer between hydrogenases and mono- and multiheme cytochromes in *Desulfovibrio* ssp. J. Biol. Inorg. Chem. *3*, 494–498.

9. Aubert, C., Brugna, M., Dolla, A., Bruschi, M., and Giudici-Orticoni, M.T. (2000). A sequential electron transfer from hydrogenases to cytochromes in sulfate-reducing bacteria. Biochim. Biophys. Acta *1476*, 85–92.
10. Rossi, M., Pollock, W.B., Reij, M.W., Keon, R.G., Fu, R., and Voordouw, G. (1993). The hmc operon of *Desulfovibrio vulgaris* subsp. *vulgaris* Hildenborough encodes a potential transmembrane redox protein complex. J. Bacteriol. *175*, 4699–4711.
11. Dolla, A., Pohorelic, B.K., Voordouw, J.K., and Voordouw, G. (2000). Deletion of the hmc operon of *Desulfovibrio vulgaris* subsp. *vulgaris* Hildenborough hampers hydrogen metabolism and low-redox-potential niche establishment. Arch. Microbiol. *174*, 143–151.
12. Florens, L., Ivanova, M., Dolla, A., Czjzek, M., Haser, R., Verger, R., and Bruschi, M. (1995). Interfacial properties of the polyheme cytochrome c_3 superfamily from *Desulfovibrio*. Biochemistry *34*, 11327–11334.
13. Higuchi, Y., Yagi, T., and Voordouw, G. (1994). Hexadecaheme cytochrome c. Methods Enzymol. *243*, 155–165.
14. Czjzek, M., Arnoux, P., Haser, R., and Shepard, W. (2001). Structure of cytochrome c_7 from *Desulfuromonas acetoxidans* at 1.9 Å resolution. Acta Crystallogr. D Biol. Crystallogr. *57*, 670–678.
15. Matias, P.M., Saraiva, L.M., Soares, C.M., Coelho, A.V., LeGall, J., and Carrondo, M.A. (1999). Nine-haem cytochrome c from *Desulfovibrio desulfuricans* ATCC 27774: primary sequence determination, crystallographic refinement at 1.8 Å and modelling studies of its interaction with the tetrahaem cytochrome c_3. J. Biol. Inorg. Chem. *4*, 478–494.
16. Matias, P.M., Coelho, R., Pereira, I.A., Coelho, A.V., Thompson, A.W., Sieker, L.C., Gall, J.L., and Carrondo, M.A. (1999). The primary and three-dimensional structures of a nine-haem cytochrome c from *Desulfovibrio desulfuricans* ATCC 27774 reveal a new member of the Hmc family. Structure *7*, 119–130.
17. Umhau, S., Fritz, G., Diederichs, K., Breed, J., Welte, W., and Kroneck, P.M. (2001). Three-dimensional structure of the nonaheme cytochrome c from *Desulfovibrio desulfuricans* Essex in the Fe(III) state at 1.89 Å resolution. Biochemistry *40*, 1308–1316.
18. Vignais, P.M., Billoud, B., and Meyer, J. (2001). Classification and phylogeny of hydrogenases. FEMS Microbiol. Rev. *25*, 455–501.
19. Coutinho, I.B., and Xavier, A.V. (1994). Tetraheme cytochromes. Methods Enzymol. *243*, 119–140.
20. Page, C.C., Moser, C.C., Chen, X., and Dutton, P.L. (1999). Natural engineering principles of electron tunnelling in biological oxidation-reduction. Nature *402*, 47–52.
21. Barker, P.D., and Ferguson, S.J. (1999). Still a puzzle: why is haem covalently attached in c-type cytochromes? Structure *7*, R281–290.
22. Florens, L., Bianco, P., Haladjian, J., Bruschi, M., Protasevich, I., and Makarov, A. (1995). Thermal stability of the polyheme cytochrome c_3 superfamily. FEBS Lett. *373*, 280–284.
23. Andersson, K.K., Lipscomb, J.D., Valentine, M., Munck, E., and Hooper, A.B. (1986). Tetraheme cytochrome c_{554} from *Nitrosomonas europaea*. Heme-heme interactions and ligand binding. J. Biol. Chem. *261*, 1126–1138.
24. Igarashi, N., Moriyama, H., Fujiwara, T., Fukumori, Y., and Tanaka, N. (1997). The 2.8 Å structure of hydroxylamine oxidoreductase from a nitrifying chemoautotrophic bacterium, *Nitrosomonas europaea*. Nat. Struct. Biol. *4*, 276–284.
25. Kimura, K., Nakahara, Y., Yagi, T., and Inokuchi, H. (1979). Electrical conduction of hemoprotein in the solid phase: anhydrous cytochrome c_3 film. J. Chem. Phys. *70*, 3317–3323.
26. Dolla, A., Guerlesquin, F., Bruschi, M., and Haser, R. (1991). Ferredoxin electron transfer site on cytochrome c_3. Structural hypothesis of an intramolecular electron transfer pathway within a tetra-heme cytochrome. J. Mol. Recognit. *4*, 27–33.
27. Matias, P.M., Frazao, C., Morais, J., Coll, M., and Carrondo, M.A. (1993). Structure analysis of cytochrome c_3 from *Desulfovibrio vulgaris* Hildenborough at 1.9 Å resolution. J. Mol. Biol. *234*, 680–699.
28. Iverson, T.M., Arciero, D.M., Hsu, B.T., Logan, M.S., Hooper, A.B., and Rees, D.C. (1998). Heme packing motifs revealed by the crystal structure of the tetra-heme cytochrome c_{554} from *Nitrosomonas europaea*. Nat. Struct. Biol. *5*, 1005–1012.
29. Czjzek, M., Guerlesquin, F., Bruschi, M., and Haser, R. (1996). Crystal structure of a dimeric octaheme cytochrome c_3 (M(r) 26,000) from *Desulfovibrio desulfuricans* Norway. Structure *4*, 395–404.
30. Deisenhofer, J., Epp, O., Miki, K., Huber, R., and Michel, H. (1984). X-ray structure analysis of a membrane protein complex. Electron density map at 3 Å resolution and a model of the chromophores of the photosynthetic reaction center from *Rhodopseudomonas viridis*. J. Mol. Biol. *180*, 385–398.
31. Morelli, X., Dolla, A., Czjzek, M., Palma, P.N., Blasco, F., Krippahl, L., Moura, J.J., and Guerlesquin, F. (2000). Heteronuclear NMR and soft docking: an experimental approach for a structural model of the cytochrome c_{553}-ferredoxin complex. Biochemistry *39*, 2530–2537.
32. Morelli, X., Czjzek, M., Hatchikian, C.E., Bornet, O., Fontecilla-Camps, J.C., Palma, N.P., Moura, J.J., and Guerlesquin, F. (2000). Structural model of the Fe-hydrogenase/cytochrome c_{553} complex combining transverse relaxation-optimized spectroscopy experiments and soft docking calculations. J. Biol. Chem. *275*, 23204–23210.
33. Morelli, X.J., Palma, P.N., Guerlesquin, F., and Rigby, A.C. (2001). A novel approach for assessing macromolecular complexes combining soft-docking calculations with NMR data. Protein Sci. *10*, 2131–2137.
34. Palma, P.N., Krippahl, L., Wampler, J.E., and Moura, J.J. (2000). BiGGER: a new (soft) docking algorithm for predicting protein interactions. Proteins *39*, 372–384.
35. Williams, P.A., Fülöp, V., Leung, Y.-C., Chan, C., Moir, J.W.B., Howlett, G., Ferguson, S.J., Radford, S.E., and Hajdu, J. (1995). Pseudospecific docking surfaces on electron transfer proteins as illustrated by pseudoazurin, cytochrome c_{550} and cytochrome cd_1 nitrite reductase. Nat. Struct. Biol. *2*, 975–982.
36. ElAntak, L., Morelli, X., Bornet, O., Hatchikian, C., Czjzek, M., Dolla, A., and Guerlesquin, F. (2002). The cytochrome c_3-[Fe] hydrogenase electron transfer complex: structural model by NMR restrained soft docking. Submitted.
37. Bruschi, M., Hatchikian, C.E., Golovleva, L.A., and Gall, J.L. (1977). Purification and characterization of cytochrome c_3, ferredoxin, and rubredoxin isolated from *Desulfovibrio desulfuricans* Norway. J. Bacteriol. *129*, 30–38.
38. Ottwinowski, Z. (1993). DENZO: "An Oscillation Data Processing Program for Macromolecular Protein" (New Haven, CT: Yale University Press).
39. CCP4 (Collaborative Computational Project 4) (1994). The CCP4 suite: programs for protein crystallography. Acta Crystallogr. *D 50*, 760–763.
40. De La Fortelle, E., and Bricogne, G. (1997). Macromolecular crystallography. In Methods in Enzymology, Volume 276, C.W. Carter, Jr., and R.M. Sweet, eds. (New York: Academic Press), pp. 472–494.
41. Roussel, A., and Cambillau, C. (1991). TURBO-FRODO: A Tool for Building Structural Models. (Mountain View, CA: Silicon Graphics).
42. ElAntak, L., Bornet, O., Morelli, X., Dolla, A., and Guerlesquin, F. (2002). Sequential NMR assignment of the ferri-cytochrome c_3 from *Desulfovibrio vulgaris* Hildenborough. J. Biomol. NMR *23*, 69–70.
43. Kraulis, P. (1991). MOLSCRIPT: a program to produce both detailed and schematic plots of protein structures. J. Appl. Crystallogr. *24*, 946–950.
44. Merritt, E.A., and Murphy, M.E.P. (1994). Raster3D version 2.0. A program for photorealistic molecular graphics. Acta Crystallogr. *D50*, 869–873.

Accession Numbers

Coordinates and structure factors have been deposited in the Protein Data Bank under ID code 1gws.